Kondo effect of cobalt adatoms on nanostructured Cu-O surfaces: Scanning tunneling spectroscopy experiments and first-principles calculations

A. Gumbsch,[1] G. Barcaro,[2] M. G. Ramsey,[1] S. Surnev,[1] A. Fortunelli,[2,*] and F. P. Netzer[1,†]
[1]*Institute of Physics, Surface and Interface Physics, Karl-Franzens University Graz, A-8010 Graz, Austria*
[2]*Molecular Modeling Laboratory, Istituto per i Processi Chimico-Fisici (IPCF), CNR, v. G. Moruzzi 1, 56124 Pisa, Italy*
(Received 11 November 2009; revised manuscript received 7 March 2010; published 12 April 2010)

The Kondo response of single Co adatoms on a nanostructured Cu(110)-O stripe phase is studied using scanning tunneling spectroscopy (STS) and first-principles calculations. The nanostructured Cu-O substrate consists of a regular array of clean Cu(110) and oxygen-reconstructed Cu(110) 2×1-O stripes and allows us to measure STS of Co adatoms in different chemical environments under identical experimental conditions. The characteristic Kondo parameters are obtained from the Fano line-shape analysis of the STS data, finding a qualitatively different behavior on clean Cu(110) and Cu(110) 2×1-O adsorption sites, with a Fano-type peak around the Fermi energy in STS on Cu(110) and a Fano dip on Cu(2×1)-O, and mean Kondo temperatures of ~125 K and ~93 K, respectively. Density-functional calculations are performed to reveal the detailed geometry and the electronic structure of the Co adsorption complexes, and are used in conjunction with simple models of the Kondo effect to rationalize the present experimental observations and the trends with respect to literature data on other Cu surfaces.

DOI: 10.1103/PhysRevB.81.165420 PACS number(s): 72.10.Fk, 68.37.Ef, 72.15.Qm, 68.43.−h

I. INTRODUCTION

The interaction of the conduction-band electrons of a nonmagnetic host metal with the localized spins of an embedded magnetic impurity atom gives rise to spin-flip scattering processes, which at sufficiently low temperatures create a correlated many-body singlet ground state forming a narrow Abrikosov-Suhl resonance in the local density of states of the impurity around the Fermi energy. This is the spectroscopic fingerprint of the Kondo effect,[1] formulated some 45 years ago to explain the previously observed anomalous transport properties at low temperatures in simple metals containing magnetic impurities.[2,3] Although the Kondo phenomenon as a prototypical example of correlation effects in condensed-matter physics has remained of interest in the following years, quantitative theoretical predictions of the properties of the Kondo many-body ground state from first principles are still under debate. Empirical Hamiltonians able to capture the basic physics of the Kondo phenomena have been proposed[4–6] but the quantitative connection between the parameters of these Hamiltonians and the complicated electronic picture obtained from sophisticated first-principles calculations still remains elusive, due to the intrinsically many-body character of the underlying physics and the complexity of the systems in which the Kondo effect is realized. The Kondo effect has received new actuality by the recent advances in experimental nanoscale techniques, in particular, in scanning tunneling microscopy (STM) and scanning tunneling spectroscopy (STS), which enabled the observation of the effect down to the single atom level. The Abrikosov-Suhl or Kondo resonances, as they are generally called, of single magnetic adatoms on surfaces of nonmagnetic metals have been first observed as sharp asymmetric features around the Fermi energy in STS spectra on Ag(111) and Au(111) surfaces.[7,8] The spectral features obtained in the STS spectra taken on top of the magnetic adatoms are often described by Fano line shapes,[9] which are interpreted by the interference between two electron-tunneling channels, one direct tunneling channel through the resonance localized at the magnetic impurity and an indirect channel into the conduction band of the metal substrate. The form and asymmetry parameter q of the Fano line shape depends on the relative strengths of direct and indirect channels whereas the half width at half maximum Γ is related to the so-called Kondo temperature T_K, which is characterized by the binding energy of the screened, many-body singlet ground state.[10]

The Kondo states of single Co adatoms on Cu(100) and Cu(111) surfaces have been studied by STS in the group of Kern *et al.*[11–13] The spectroscopic Kondo fingerprints of the Co adatoms on Cu(100) and (111) surfaces consist of characteristic Fano dips around the Fermi level, as they have been observed on most other noble-metal surfaces.[10] Schneider *et al.*[13] have suggested a simple scaling behavior of the Kondo temperature with the number of nearest-neighbor substrate atoms: increasing the coordination number n in the particular adsorption site increases T_K. In accord with the latter, for the case of Co on Cu(111), $n=3$ and $T_K\approx54$ K whereas on Cu(100), $n=4$ and $T_K\approx88$ K. The rationale behind this scaling relation is that the Kondo temperature depends on the hybridization between the adatom and the substrate electronic states which increases with the number of nearest neighbors on the supporting surface. However, a fully satisfactory atomistic understanding of the Kondo phenomenon has not been yet achieved, even though several approaches ranging from mapping onto Anderson impurity models[14] to quantum Monte Carlo methods[15] have been proposed in the literature. A route for connecting first-principles calculations to geometry-dependent empirical models, then solved via numerical renormalization-group techniques, and thus leading to explicit conductance calculations has been very recently proposed[16] but this approach has been so far demonstrated on a very simple model system, and its application to those considered in the present work, exhibiting a complex band structure and several open inter-

action channels, does not seem straightforward. Issues such as the dependence of the shape and position of the Kondo resonance on the coordination geometry of the impurity, and simple rules of thumb for predicting trends and behavior as a function of the chemical variables are therefore still under debate.[10] Some work even question the mere possibility of such a qualitative understanding.[17]

In this context, enlarging the scope of the investigated systems to novel but well-characterized geometries and coordination environments together with an accompanying analysis conducted at the computational level seems useful to realize further progress. Interestingly, no experiments of the Kondo effect have been reported for magnetic adatoms on the more open low-index surfaces of metals, such as, e.g., the fcc (110) surfaces. The adsorption sites in the troughs of the (110) surface support higher coordination numbers, and according to simplistic models,[13] higher Kondo temperatures might be expected. In the present work, we have chosen to investigate the Kondo effect of single Co adatoms on a nanostructured Cu-O surface, which is based on a Cu(110) template. Under suitable conditions of oxygen pressure and of the Cu(110) substrate temperature, a regular Cu-O "stripe" phase develops in which regions of the Cu-O (2×1) surface reconstruction self-assemble into nanoscopic Cu-O stripes separated by stripes of the clean Cu(110) surface[18–20] [see Fig. 1(a)]. The Cu(110)2×1-O reconstructed surface layer is somewhat related to the Cu_2N copper nitride on Cu(100), which has also been investigated as a substrate for single-atom Kondo measurements.[21] However, the Cu nitride layer is more closed than the Cu-O layer and thus decouples the Co adatoms more effectively from the metal than the Cu-O layer. The present Cu-O nanostructured substrate system allows us to measure the Kondo behavior of Co adatoms under the same experimental conditions on a surface with two different chemical environments and different adatom-substrate coupling strengths. Thus we are able to examine how the local chemical environment of the adatom determines its magnetic properties. We have recorded the STM images and STS spectra in a low-temperature (~5 K) scanning tunneling microscope and the experimental observations are supplemented by first-principles density-functional (DF) calculations.

As an interesting qualitative observation we report that the Kondo resonance in STS of Co adatoms on Cu(110) is characterized by a *peak* around the Fermi energy, in contrast to the reported dips on most other noble-metal surfaces.[10] This together with the scaling behavior of T_K and the position of the resonance with the adsorption geometry and the adsorbate chemical bonding will be discussed comparatively with reference to results in the literature from Cu(100) and Cu(111) surfaces in the light of DF local density of states (LDOS) calculations of the adsorbate complexes. The detailed knowledge of the adsorption geometry and the electronic structure of the investigated systems as derived from DF results will allow us to discuss the experimentally observed trends in terms of simple arguments.

II. EXPERIMENTAL AND COMPUTATIONAL DETAILS

The STM/STS experiments have been carried out in a three-chamber low-temperature STM system (CreaTec, Germany) in ultrahigh vacuum (UHV) with a base pressure of $\sim5\times10^{-11}$ mbar, operated at a measurement temperature of ~5–6 K in the liquid He STM cryostat stage.[22] Sample surface cleaning and preparation and *in situ* STM tip treatments are performed in the preparation chamber, which is equipped with a liquid He coolable manipulator (reaching sample temperatures of ~15–20 K), a LEED optics, a mass spectrometer, evaporation sources, a quartz microbalance in a position suitable for monitoring evaporation rates, and the usual provisions for surface cleaning and controlled gas inlet. The samples can be transferred cold into the STM stage directly from the cooled manipulator. A small fast-entry chamber for quick sample and tip exchanges via a magnetically coupled transfer device completes the STM system. Electrochemically etched W tips have been treated *in situ* by electron bombardment heating, by field emission via voltage pulses, and by controlled dipping into the Cu substrate. Spectroscopy of the differential conductance (dI/dV) was performed by a lock-in technique with 1.1 kHz modulation frequency and typically a 5 mV pp modulation amplitude. The voltages quoted are sample potentials with respect to the tip, the typical tip feedback loop set point for STS was 10 mV, 1 nA.

The Cu(110) surface was cleaned by standard techniques, i.e., Ar^+-ion sputtering (700 eV) and annealing (825 K)

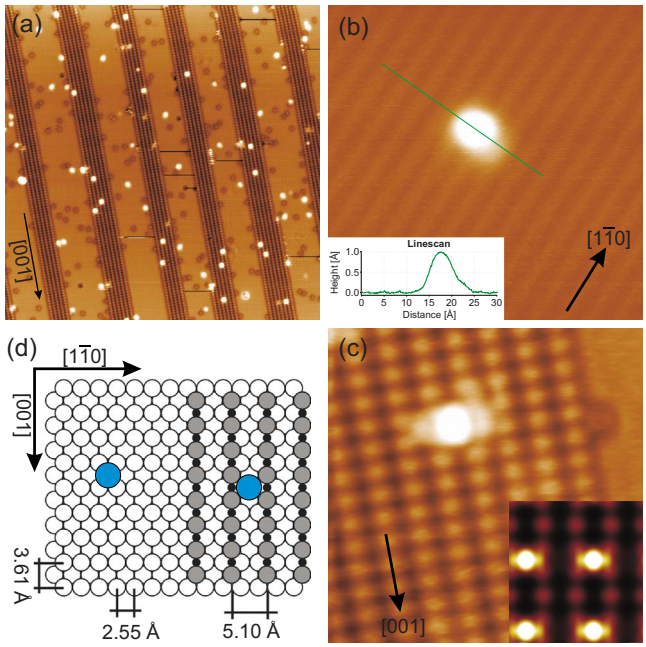

FIG. 1. (Color online) (a) Constant current topographic STM image of the Cu(110)(2×1)-O stripe phase, displaying bare Cu(110) and Cu-(2×1)-O stripes (with darker contrast), covered with $\sim10^{-3}$ monolayer of cobalt adatoms (bright contrast) (400 $\times400$ Å^2; tunneling conditions: 100 mV sample bias; 0.4 nA tunneling current). (b) High-resolution STM image of a single Co adatom on clean Cu(110) (48×48 Å^2; 1 V, 1 nA). The inset shows a scan along the dark line across the Co adatom. (c) High-resolution STM image of a single Co adatom on the Cu(110)(2×1)-O reconstructed surface (48×48 Å^2; 1 V, 0.6 nA). The inset shows a DFT-simulated STM image of Co adatoms on Cu-O. (d) Schematic model of Cu(110) (left) and Cu(110)(2×1)-O (right) with Co adatoms, specifying the Co adsorption sites. Co atoms are in dark grey (blue in color) and Cu-O rows in grey (dark grey in color).

TABLE I. Distances r_{ij} of Cu neighbors from Co adatoms, average Fano fit parameters q, δ, Γ, and average Kondo temperature T_K.

Substrate	r_{ij} (Å)	q	δ (meV)	Γ (meV)	T_K (K)
Cu(110)	4×2.448 1×2.238	$\in[10;10^6]$	6.9 ± 2.1	10.8 ± 2.6	125 ± 30
Cu(110)-(2×1)O	4×2.888 2×2.527	$\in[-1;0]$	8.9 ± 3.0	8.0 ± 0.7	93 ± 8

cycles in UHV. The Cu(110)(2×1)-O stripe phase was prepared by dosing 0.5–1.5 L [1 Langmuir (L)=1 $\times10^{-6}$ torr s] O_2 at a sample temperature of 600 K followed by annealing (600 K) in UHV for 1 min. Co adatoms (typical coverages some 10^{-3} monolayers) were deposited using an electron-beam evaporator onto the cold substrate surface on the cooled manipulator ($\sim$15–20 K) in the preparation chamber. Some depositions were also performed at $\sim$5–10 K directly into the STM stage but the results obtained were strictly similar in the two cases.

DF calculations were performed using the PWSCF (plane-wave self-consistent field) computational code,[23] employing ultrasoft pseudopotentials[24] and the PBE exchange-correlation functional.[25] A value of 40 Ry as the energy cutoff for the selection of the plane-wave basis set for the description of the wave function and of 240 Ry for the description of the electronic density were employed. The metal support was described using seven layers and considering a symmetric adsorption of a cobalt atom on both sides of the metallic slab (to cancel the dipole moment of the system). The atoms of the innermost three layers were kept fixed in the positions of bulk fcc crystal (a lattice constant corresponding to a first-neighbor distance of 2.58 Å was chosen, corresponding to the equilibrium value of bulk Cu predicted by the present DF approach) whereas the positions of the outer two layers on each side, as well as the coordinates of the cobalt atoms, were fully optimized until the forces were smaller than 0.01 eV/Å per atom. All the calculations were performed spin unrestricted. The dimensions of the unit cell along the surface (xy plane) were chosen as to maintain a minimum distance between Co atoms in replicated vicinal cells of about 7 Å. The first Brillouin zone was k sampled employing a (221) mesh, and a Gaussian smearing of each level of about 0.03 eV.

III. RESULTS AND DISCUSSION

Figure 1(a) shows a wide scan constant current topographic STM image of the Cu(110)(2×1)-O stripe surface covered with a small amount of Co adatoms (coverage $\sim10^{-3}$ monolayer), deposited at 15 K and imaged at $\sim$5 K. The dark stripes, $\sim$25 Å of average width and displaying a clear atomic line contrast, correspond to the Cu-O rows of the (2×1) reconstruction running along the [001] direction. The Co adatoms are visible with a bright contrast and are evenly distributed over the Cu and Cu-O stripes, no preferential nucleation is observed. High-resolution STM topographs of single Co adatoms on clean Cu and on Cu (2×1)-O stripes are displayed in Figs. 1(b) and 1(c), respectively. It is recognized that the Co adatoms are located in the troughs of the surface in both regions, between the bare Cu rows along $[1\bar{1}0]$ [Fig. 1(b)] or between the Cu-O rows along [001] [Fig. 1(c)]. The schematic model of the clean Cu(110) and Cu(110)(2×1)-O regions in Fig. 1(d) specifies the adsorption geometries of the Co adatoms. DF calculations in which several adsorption sites were tested and fully geometry relaxations were performed indicate that on clean Cu(110) [left-hand side of Fig. 1(d)], the Co adatoms in the most stable configuration have four nearest-neighbor Cu atoms in the first-layer and a further second-layer Cu atom directly below the Co adatom, at a close distance of $\sim$2.24 Å; the adsorption site may therefore be regarded as being fivefold coordinated. On the Cu-O reconstruction, the situation is more complex, with four nearest-neighbor Cu atoms and two oxygen atoms in the first reconstructed layer and two Cu atoms in the layer below, where the Co adatoms occupy bridge sites. The inset in Fig. 1(c) displays a simulated STM image of Co on Cu-O in the calculated adsorption site; we note the excellent agreement with the experimental image. The distances r_{ij} between the Co adatoms and their neighboring Cu atoms as calculated by DF are included in Table I.

Representative STS spectra taken from the Cu(110)(2×1)-O stripe surface on top of Co adatoms and on the bare substrate regions are presented in Fig. 2. The uppermost spectrum is from the top of a Co adatom on Cu(110): it shows a pronounced peak in the vicinity of the Fermi energy E_F (=0 V sample bias). The bottom spectrum has been recorded on top of a Co adatom on the Cu-O reconstruction: here, a clear dip is observed. The STS spectrum from the clean Cu(110) substrate (second curve from top) shows no significant spectral feature around E_F and so does the STS spectrum from the bare Cu-O reconstruction (third curve from top).

As mentioned in Sec. I, the form of the Kondo resonance in the STS spectra may be described by a Fano line function,[9,10]

$$(dI/dV)(V)\alpha(q+\varepsilon)^2/(1+\varepsilon^2)+c \qquad (1)$$

with the normalized energy $\varepsilon=(eV-\delta)/\Gamma$ and a constant c. The parameters q, δ, and Γ are fit parameters for the experimental data and signify the asymmetry parameter q, the energy shift δ of the Kondo resonance from zero bias (i.e., E_F), and the half width of the feature at half maximum Γ, which is related to the characteristic Kondo temperature $T_K=\Gamma/k_B$ (k_B is the Boltzmann constant). Figure 3 displays the Fano fits of the STS data for Co on clean Cu(110) [panel (a)] and for Co on Cu(110)(2×1)-O [panel (b)]. The data in Fig. 3

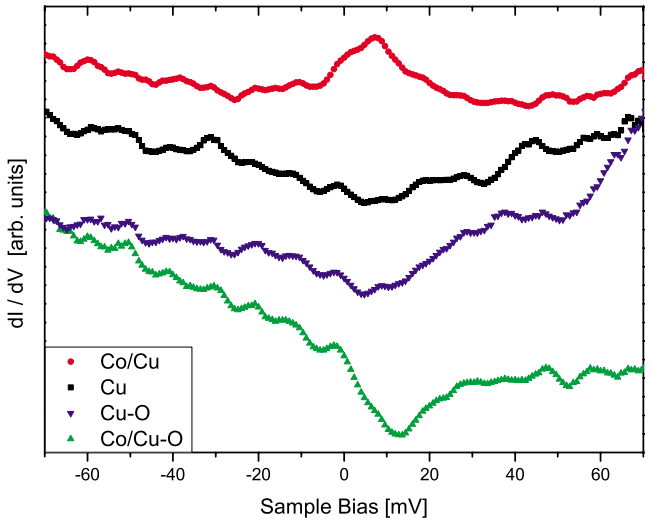

FIG. 2. (Color online) Differential conductance STS spectra (dI/dV versus V) from the Cu(110)(2×1)-O stripe phase. Top curve: STS on top of a Co adatom on clean Cu(110); middle curves: STS from clean Cu(110) and bare Cu(110)2×1-O, respectively; bottom curve: STS on top of a Co adatom on Cu(110)(2×1)-O. STS set point: 10 mV, 1 nA.

have been background corrected before fitting, that is the corresponding STS spectra of the bare substrates, recorded in the same experimental run with strictly the same tip conditions, have been subtracted directly without normalization from the raw spectra (such as those shown in Fig. 2). The average Fano fit parameters obtained from the analysis of a large set of data are given in Table I. Notably, two major differences are recognized in the Kondo response of Co adatoms on Cu(110) and on Cu(110)(2×1)-O: on Cu(110) Fano peaks with $T_K \approx 125 \pm 30$ K, and on Cu-(2×1)-O Fano dips with $T_K \approx 93 \pm 8$ K have been derived. Thus, the different chemical environment of the Co adsorption sites on the two substrates is evidently reflected in a qualitatively different Kondo behavior. This will be discussed in the following in comparison with previous results from the literature and in the light of the present LDOS DF calculations.

In current models of the Kondo effect,[10,26–28] the Fano line shape is understood by the interference between two electron-tunneling channels between the tip and the surface: one direct channel coupling the tip to the impurity d level and an indirect channel coupling the tip to the substrate conduction band (we note, however, that other models not involving a direct channel have also been proposed in the literature[29,30]). Within these models, the q parameter is proportional to the ratio between the two tunneling processes,

$$q = t_2/(2\pi\rho_0\Delta t_1), \tag{2}$$

where t_2 and t_1 are matrix elements for the tip-to-impurity and the tip-to-substrate tunneling processes, respectively, ρ_0 is the density of states of the supporting metal at the Fermi level, and Δ is the hybridization matrix element that couples the localized state with the continuum of band states (or, more precisely, an average of Δ over the various k states of the conduction band). The difficulty is in extracting information on the t_2/t_1 ratio from first-principles simulations. The DF method, being a mean-field approach, does not take fully into account electronic correlation effects, and predicts, for example, a finite nonzero magnetic moment instead of a spin-zero ground state for the system. Nevertheless, it is interesting to discuss the electronic band structure of the systems, and, in particular, the PDOS, in more detail. In Figs. 4(a) and 4(b), the LDOS projected onto Co orbitals vs energy for Co adatoms on the Cu(110) and Cu(110)(2×1)-O surfaces are shown. The number of electrons in majority- and minority-spin bands obtained via a Lowdin charge analysis is also reported: note that the net spin polarization is around 2, corresponding to two impurity orbitals or a two-channel Kondo system. It can be noted that in the case of Cu(110)(2×1)-O, one finds a very low density of Co $3d$ states at the Fermi level. For comparison, we performed

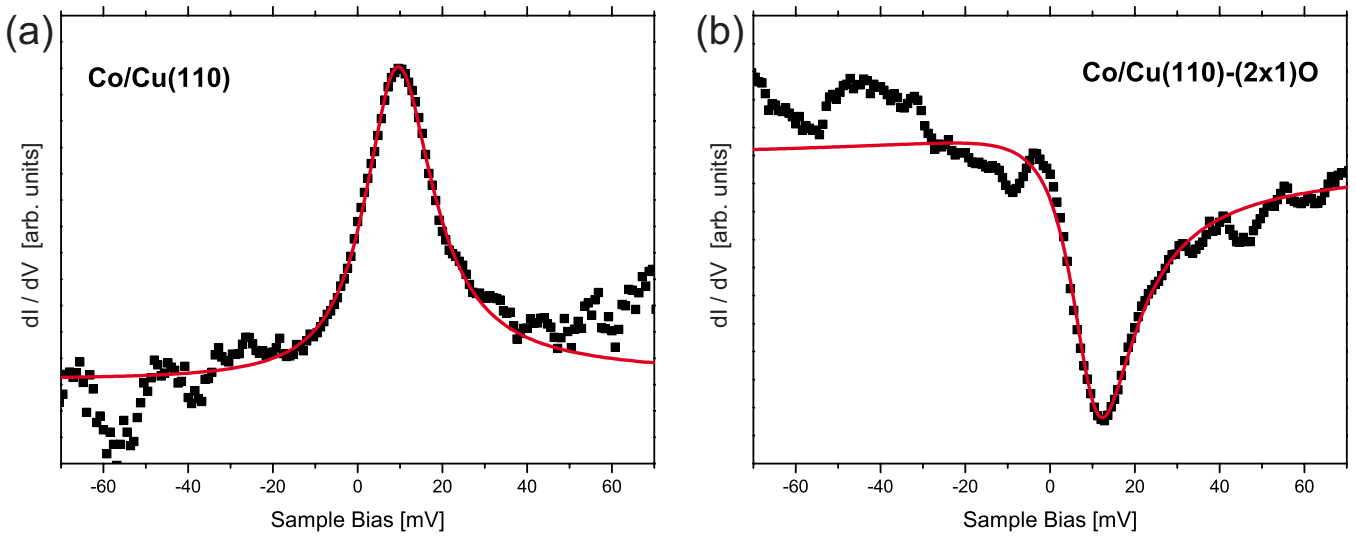

FIG. 3. (Color online) Fano line-shape fits to the STS spectra of Co on clean (a) Cu(110) and of Co on (b) Cu(110)(2×1)-O. The spectra have been processed by subtracting the background of the bare substrates before fitting. The corresponding fit parameters are given in Table I.

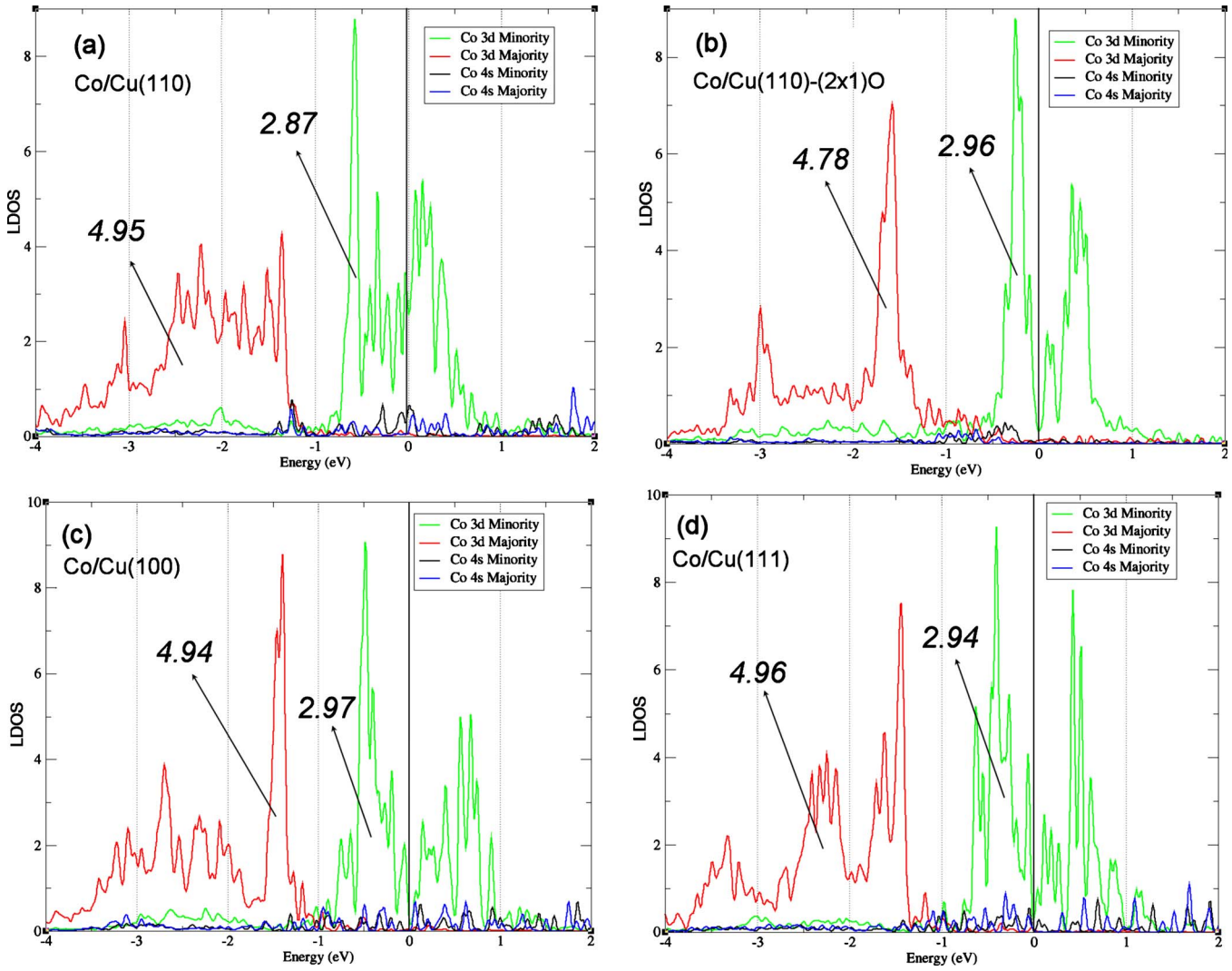

FIG. 4. (Color online) LDOS (arbitrary units) projected onto Co orbitals for Co adatoms adsorbed on (a) Cu(110), (b) Cu(110)(2 $\times$ 1)-O, (c) Cu(100), and (d) Cu(111) substrates in an energy window of $[-4.0-2.0]$ eV. The Fermi energy (full line) is at 0 eV. The values pointed by arrows correspond to the number of electrons in the Co 3*d* bands: majority (red) and minority (dark green) spin, respectively.

analogous DF calculations for the adsorption of a Co adatom on Cu(100) and Cu(111) substrates, using an identical structural setup (see the computational details in Sec. II) and numerical parameters. The LDOS plots [shown in Figs. 4(c) and 4(d)] are entirely analogous to the Cu(110)(2$\times$1)-O case, and it is interesting to note that a Fano dip is found for those systems in the STS experiments of Refs. 11–13. In the case of Co/Cu(110), instead, one finds in Fig. 4(a), a high density of Co 3*d* states at the Fermi level. This difference, between the bare Cu(110) substrate on the one side and the Cu(110)(2$\times$1)-O and the other bare Cu substrates on the other side, results from the circumstance that when a Co atom is adsorbed on the Cu(110)(2$\times$1)-O surface, as well as on Cu(100) and Cu(111), the *d* orbitals of Co are well split by the crystal field into a lower band comprising three orbitals and an upper band comprising two orbitals; in this way, the Fermi energy falls into a minimum of the Co *d* LDOS whereas on the Cu(110) surface, the crystal field is reversed and the Fermi energy falls into the middle of the Co *d* LDOS. Without being able to make definite predictions, we thus observe an interesting correlation between Fano line shape and Co 3*d* PDOS at the Fermi level.

An important parameter in the quantitative analysis of the Kondo resonance is the Kondo temperature T_K. As the application of recently proposed approaches to link DF calculations to solvable empirical models and thus to actual predictions of spectral features[16] seems still unfeasible for such complicated systems as those here considered, we will try to single out some qualitative trends with the help of analytic model formulas. We use the equation (derived in the weak-coupling limit of the s-d model[4] via the Schrieffer-Wolff transformation[6,31]),

$$k_B T_K = [(U\Delta)/2]^{1/2} \exp[-\pi/(2U\Delta) \cdot |\varepsilon_d| \cdot |\varepsilon_d + U|], \quad (3)$$

where Δ is the hybridization matrix element that couples the localized state with the continuum of band states as above, U is the on-site Coulomb repulsion, and ε_d is the position of the impurity *d* level with respect to the Fermi energy. We then assume that U and ε_d are roughly constant, and linearize T_K

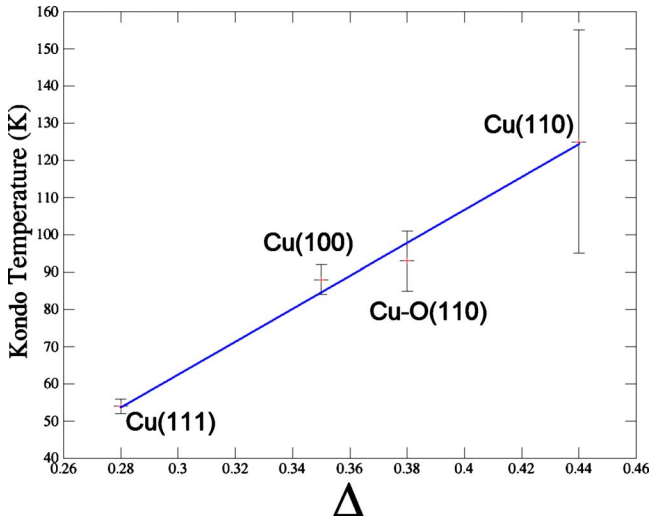

FIG. 5. (Color online) Kondo temperature T_K (experimental values in kelvin from the present work and Ref. 12) vs Δ, derived from the present DF calculations for Co adatoms on different Cu substrates. Δ is related to the coordination number of the Co impurity atom.

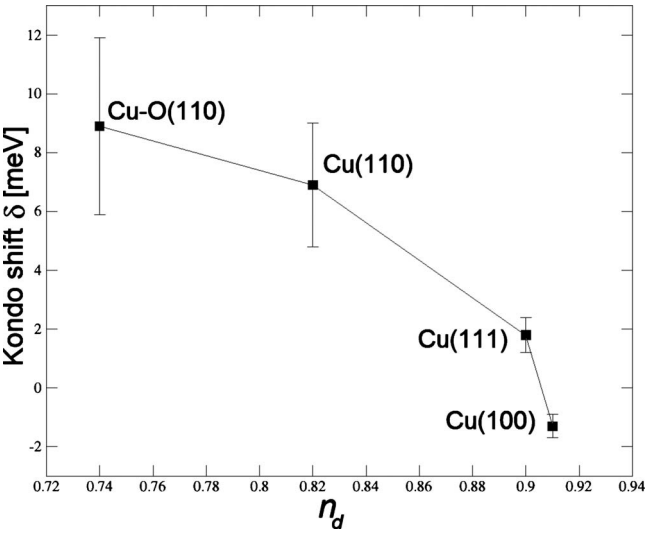

FIG. 6. Shift, δ, of the Kondo resonance in millielectron volt with respect to the Fermi energy (experimental values from the present work and Ref. 12) as a function of the occupation number of the $3d$ states, n_d, of a Co adatom on the four substrates considered in the present work. n_d is calculated according to Eq. (6) (see text).

as a function of Δ (which is legitimate as Δ varies in a narrow range). In other words, we assume that the width of the resonance is mainly determined by the intrinsic coupling (Δ) between the discrete state and the conduction-electron continuum. Moreover, since Δ is related to the broadening of the impurity state, it can be assumed to be roughly proportional to the number of Cu neighbors multiplied by an exponentially decreasing matrix element,[12]

$$\Delta \approx \Sigma_{j\text{th Cu neighbor}} \exp(-r_{ij}) \tag{4}$$

with r_{ij} the distance of the jth Cu neighbor from the Co impurity atom, evaluated from the DF local energy minimizations and reported explicitly in Table I for the Cu(110) substrates. The plot of T_K as a function of the approximate Δ, including Cu(100) and Cu(111) substrates whose experimental data are taken from Ref. 12, is shown in Fig. 5, in which a linear relationship between the two quantities can be observed. Note that T_K assumes its maximum value on the Cu(110) substrate on which the maximum coordination number is also realized but that a precise definition of the adsorption geometry, as allowed by the DF approach, is necessary to rationalize the value of T_K for the Cu(110)(2×1)-O substrate.

The last quantity that can be extracted from experimental data is the position δ of the Kondo resonance. This is related to the occupation number n_d of the $3d$ states of the adatom on the surface[31] by the relation,

$$\delta = \Gamma \tan[\pi/2(1-n_d)]. \tag{5}$$

The average occupation number n_d depends on the charge transfer between the host metal and the impurity, and ranges between $n_d=0$ for an empty and $n_d=2$ for a doubly occupied orbital, where the Kondo régime is roughly $0.8<n_d<1.2$, with approximately one unpaired electron in the impurity d level. n_d can be estimated from the DF wave functions via a Lowdin projection as

$$n_d = n_{d,\alpha} + n_{d,\beta} - 7, \tag{6}$$

where $n_{d,\alpha}$ and $n_{d,\beta}$ are the average numbers of electrons in the Co $3d$ majority- and minority-spin bands, respectively. In Fig. 6, the values of δ for the four systems under consideration are plotted as a function of n_d, where the values of δ for Co/Cu(100) and Co/Cu(111) are taken from Ref. 12. In qualitative agreement with Eq. (5), the Kondo shift δ increases with decreasing occupation number n_d, reaching its maximum for the oxidized Cu(110)(2×1)-O system, even though an accurate interpolation is not possible, also due to uncertainties in the δ values and to the approximate values of n_d derived from Lowdin occupations. In connection with the last point, it can be noted that atomic occupations are not physical observables, and that n_d values different from those derived from Lowdin occupations can be obtained using other approaches for projecting the one-electron states onto atomic orbitals. However, we do not expect that these other possible choices would spoil the fair correlation displayed in Fig. 6.

IV. CONCLUSIONS

The spin interaction of single Co adatoms with the conduction electrons of a clean Cu(110) and of an oxygen-reconstructed Cu(110)2×1-O surface has been investigated via the Kondo resonance in scanning tunneling spectroscopy measured at 5 K on a nanostructured Cu(110)-O stripe phase. The Kondo response of the Co atoms is significantly different on the two surfaces, exhibiting a Fano peak (as observed for other systems[32]) around the Fermi energy on clean Cu(110) and a Fano dip on Cu(110)2×1-O,

thus reflecting the different chemical environment of the adsorption sites. From the Fano line-shape analysis, the parameters characterizing the Kondo effect have been determined, with a Kondo temperature $T_K = 125 \pm 30$ K on Cu(110) and $T_K = 93 \pm 8$ K on Cu(110)2×1-O. Density-functional theory has been applied to reveal the details of the adsorption geometry and of the electronic structure of the Co adsorption complexes. The experimentally observed trends in the Kondo line shape, Kondo temperature, and position of the Kondo resonance relative to E_F have been discussed with reference to results in the literature on Cu(100) and Cu(111) surfaces and have been related to the local geometry and the LDOS of the Co adatoms, applying the quantitative results of the DF calculations and qualitative arguments from simple models of the Kondo effect. While the Kondo temperature of Co on clean Cu(110) is found to scale linearly with those on the other low-index Cu surfaces in terms of the number of nearest-neighbor substrate atoms, a more refined picture of the adsorption complex as delivered by the DF calculations is necessary to interpret T_K on the O-reconstructed surface. The measured energetic position of the Kondo resonance has been semiquantitatively correlated with the average occupation number of the Co $3d$ impurity levels as estimated from the DF-calculated charge projections. Finally, we observe a correlation between the local d density of the Co adatoms at the Fermi energy and the line shapes on clean Cu(110) and Cu(110)-O surfaces.

ACKNOWLEDGMENTS

This work has been supported by the ERC Advanced Grant "SEPON" and by the Rektor of the Karl-Franzens University Graz.

*fortunelli@ipcf.cnr.it
†falko.netzer@uni-graz.at

[1] J. Kondo, Prog. Theor. Phys. **32**, 37 (1964).
[2] W. Meissner and B. Voigt, Ann. Phys. **399**, 761 (1930).
[3] W. J. de Haas, J. de Boer, and G. J. van den Berg, Physica (Utrecht) **1**, 1115 (1934).
[4] P. W. Anderson, Phys. Rev. **124**, 41 (1961).
[5] J. Kondo, Phys. Rev. **169**, 437 (1968).
[6] J. R. Schrieffer and P. A. Wolff, Phys. Rev. **149**, 491 (1966).
[7] J. Li, W.-D. Schneider, R. Berndt, and B. Delley, Phys. Rev. Lett. **80**, 2893 (1998).
[8] V. Madhavan, W. Chen, T. Jamneala, M. F. Crommie, and N. S. Wingreen, Science **280**, 567 (1998).
[9] U. Fano, Phys. Rev. **124**, 1866 (1961).
[10] M. Ternes, A. J. Heinrich, and W.-D. Schneider, J. Phys.: Condens. Matter **21**, 053001 (2009).
[11] N. Knorr, M. A. Schneider, L. Diekhöner, P. Wahl, and K. Kern, Phys. Rev. Lett. **88**, 096804 (2002).
[12] P. Wahl, L. Diekhöner, M. A. Schneider, L. Vitali, G. Wittich, and K. Kern, Phys. Rev. Lett. **93**, 176603 (2004).
[13] M. A. Schneider, L. Vitali, P. Wahl, N. Knorr, L. Diekhöner, G. Wittich, M. Vogelsang, and K. Kern, Appl. Phys. A **80**, 937 (2005).
[14] P. Roura-Bas, M. A. Barral, and A. M. Llois, Phys. Rev. B **79**, 075410 (2009).
[15] E. Gorelov, T. O. Wehling, A. N. Rubtsov, M. I. Katsnelson, and A. I. Lichtenstein, Phys. Rev. B **80**, 155132 (2009).
[16] P. Lucignano, R. Mazzarello, A. Smogunov, M. Fabrizio, and E. Tosatti, Nature Mater. **8**, 563 (2009).
[17] N. Néel, J. Kröger, R. Berndt, T. O. Wehling, A. I. Lichtenstein, and M. I. Katsnelson, Phys. Rev. Lett. **101**, 266803 (2008).
[18] K. Kern, H. Niehus, A. Schatz, P. Zeppenfeld, J. Goerge, and G. Comsa, Phys. Rev. Lett. **67**, 855 (1991).
[19] P. Zeppenfeld, M. Krzyzowski, C. Romainczyk, G. Comsa, and M. G. Lagally, Phys. Rev. Lett. **72**, 2737 (1994).
[20] P. Zeppenfeld, V. Diercks, C. Tölkes, R. David, and M. A. Krzyzowski, Appl. Surf. Sci. **130-132**, 484 (1998).
[21] A. F. Otte, M. Ternes, S. Loth, C. P. Lutz, C. F. Hirjibehedin, and A. J. Heinrich, Phys. Rev. Lett. **103**, 107203 (2009).
[22] A. Gumbsch, Ph.D. thesis, Karl-Franzens University Graz, 2010.
[23] S. Baroni, A. Del Corso, S. de Gironcoli, and P. Giannozzi, http://www.pwscf.org
[24] D. Vanderbilt, Phys. Rev. B **41**, 7892 (1990).
[25] J. P. Perdew, K. Burke, and M. Ernzerhof, Phys. Rev. Lett. **77**, 3865 (1996).
[26] O. Újsághy, J. Kroha, L. Szunyogh, and A. Zawadowski, Phys. Rev. Lett. **85**, 2557 (2000).
[27] V. Madhavan, W. Chen, T. Jamneala, M. F. Crommie, and N. S. Wingreen, Phys. Rev. B **64**, 165412 (2001).
[28] M. Plihal and J. W. Gadzuk, Phys. Rev. B **63**, 085404 (2001).
[29] J. Merino and O. Gunnarsson, Phys. Rev. B **69**, 115404 (2004).
[30] C.-Y. Lin, A. H. Castro Neto, and B. A. Jones, Phys. Rev. B **71**, 035417 (2005).
[31] A. C. Hewson, *The Kondo Problem to Heavy Fermions* (Cambridge University Press, Cambridge, England, 1993).
[32] A. Zhao, Q. Li, L. Chen, H. Xiang, W. Wang, S. Pan, B. Wang, X. Xiao, J. Yang, J. G. Hou, and Q. Zhu, Science **309**, 1542 (2005).